Journal of Inflammation Research

Dovepress
Taylor & Francis Group

Open Access Full Text Article

ORIGINAL RESEARCH

Electroacupuncture at ST36 Treatment Suppresses the Microglial Pyroptosis Through Activating α7nAChR in a Rat Model of Asphyxial Cardiac Arrest

Yuan Qin[1,*], Gangguo Ma[1,*], Xiao Xiao[1,*], Yongfei Liu[1], Zhaoyan Zhao[1], Fang Zhao[2], Fei Guo[1], Shuang Wang[1], Xude Sun[1], Changjun Gao[1]

[1]Department of Anesthesiology, Tangdu Hospital, The Fourth Military Medical University, Xi'an, Shaanxi, People's Republic of China; [2]Department of Infectious Diseases, Tangdu Hospital, The Fourth Military Medical University, Xi'an, Shaanxi, People's Republic of China

*These authors contributed equally to this work

Correspondence: Changjun Gao, Tangdu Hospital, The Fourth Military Medical University, Xi'an, Shaanxi, 710000, People's Republic of China, Email gaocj74@163.com

Background: Neuroinflammation is a critical element to cardiac arrest (CA)-induced global cerebral ischemia injury. Electroacupuncture (EA) treatment has demonstrated therapeutic potentials in both animal and clinical studies for the cerebral ischemic treatment. Nevertheless, the neuroprotective effect of electroacupuncture at ST36 (EA-ST36) in CA-induced global cerebral ischemia injury and the underlying mechanisms remains unclear.

Methods: Using a rat model of Asphyxial Cardiac Arrest, the neuroprotective effects of EA-ST36 were evaluated. Single cell RNA-seq analyses were performed to assess the genetic expression of pyroptosis in different cell types of brain. Cognitive performance was tested through the Morris water maze, while neuronal survival, microglial pyroptosis, and neuroinflammation were analyzed by immunofluorescence, flow cytometry, ELISA, and histopathological staining. An oxygen-glucose deprivation/reoxygenation (OGD/R) model of primary microglia was established to confirm the role of α7nAChR in inhibiting pyroptosis.

Results: Single-cell RNA sequencing of rat brain and immunofluorescent co-localization showed that pyroptosis is principally occurred in microglia rather than neurons, astrocytes, oligodendrocytes, or endothelial cells in CA/CPR rats. EA-ST36 treatment significantly improved spatial learning and memory in CA/CPR rats, reduced neuronal loss, and attenuated neuroinflammation. These neuroprotective effects were associated with suppressed microglial pyroptosis and decreased IL-1β and IL-18 levels. Remarkably, these neuroprotective effects were abolished by α7nAChR inhibitors. In vitro, α7nAChR activation suppressed OGD/R-induced microglial pyroptosis by inhibiting expression of NLRP3, cleaved caspase-1, and N-GSDMD, and decreased IL-1β and IL-18 levels and alleviated the neurotoxic effects of pyroptotic microglia.

Conclusion: Our study revealed that EA-ST36 exerted neuroprotective effects with a potent anti-neuroinflammatory potential by suppressing microglial pyroptosis in a rat CA/CPR model, and these anti-neuroinflammatory properties are α7nAChR-dependent.

Keywords: cardiac arrest, neuroinflammation, electroacupuncture, microglia, pyroptosis, α7nAChR

Introduction

Cardiac arrest (CA)-induced global cerebral ischemia injury is a critical cause of permanent disability and death worldwide with limited therapies. The estimated annual incidence of emergency medical services (EMS)-treated out-of-hospital cardiac arrest (OHCA) was 30.0–97.1 individuals per 100,000 population.[1] Research data showed that approximately 70% of patients with cardiac arrest/cardiopulmonary resuscitation (CA/CPR) died from brain injury.[2] Although the mechanism underlying brain injury following CA/CPR has not yet been fully elucidated, it is commonly

Received: 24 March 2025
Accepted: 26 June 2025
Published: 2 July 2025

acknowledged that neuroinflammation plays a crucial role, which is identified by glial cells activation, peripheral leukocyte infiltration, and pro-inflammatory cytokine production.[3]

Pyroptosis is a newly identified type of inflammation-associated programmed cell death.[4] Recently, studies showed that pyroptosis was critically involved in the pathophysiology of neuroinflammation caused by various types of cerebral ischemia injury.[5–7] Pyroptosis mediates proteolytic cleavage and release of inflammatory cytokine, these inflammatory cytokines propagate the consequential excessive neuroinflammatory through further activation of resting microglia and recruitment of leukocytes to infiltrate the brain.[8] How to effectively suppress the pyroptosis-fueled-neuroinflammatory response following cerebral ischemia to protect the nerves remains a largely unsolved issue.

Currently, increased studies demonstrated that stimulating the vagus nerve showed an inhibitory effect against the neuroinflammation through projecting to nucleus tractus solitarius (NTS) in the brainstem to activate α7nicotinic acetylcholine receptor (α7nAChR).[9–12] Although vagus nerve stimulation exhibits a salutary benefit in attenuated neuroinflammation, the invasive characteristics restrict the routine clinical application of this method. Based on previous studies, several acupoint have also been implicated in modulating inflammation, potentially through mechanisms involving α7nAChR activation, such as ST36 (Zusanli), LI4 (Hegu), GV20 (Baihui) and PC6 (Neiguan). As a combination of acupuncture and electric stimulation, electroacupuncture at ST36 acupoint (EA-ST36) has been recently demonstrated as a well-tolerated method of stimulating the vagus nerve to exhibit a robust anti-neuroinflammation effects through activating α7nAChR.[13] Therefore, we wonder whether the EA-ST36 treatment suppresses neuroinflammation in CA/CPR-induced global cerebral ischemia injury and the underlying mechanisms.

In this study, a Rat Model of Asphyxial Cardiac Arrest was established to investigate the therapeutic efficacy of EA-ST36. We explore whether the EA-ST36 treatment exerts a neuroprotective effect by inhibiting pyroptosis-fueled-neuroinflammatory in an α7nAChR-dependent manner against CA/CPR-induced cerebral injury.

Materials and Methods

Animals

Male adult Sprague Dawley rats weighing 280–320 g were supplied by the Fourth Military Medical University's Experimental Animal Center (Xi'an, China) and raised in a 12 h light-dark cycle and climate-controlled room (21°C–25°C and 55%–65% humidity). Rats were unrestricted access to standard food and water. Each treatment was approved by the Fourth Military Medical University's Animal Ethics Committee and the Animal Care and Use Committee and were performed in accordance with the Laboratory Animal-Guideline for ethical review of animal welfare (GB/T 358922–2018).

CA/CPR Model

The 8-min asphyxia cardiac arrest rat model was established in accordance with our previous study.[14] Before the experiment, rats were fasted without water deprivation for 12 h. After being anesthetized with pentobarbital sodium 40 mg/kg, intraperitoneally (i.p)., rats were orotracheally intubated using the laryngoscope for neonate, cannulated in the left femoral vein and artery used for drug delivery and dynamic blood pressure monitoring. Asphyxia was acquired by occlusion of the tracheal tube for 8 min. Resuscitation was implemented by thoracic compressions, mechanical ventilation (100% O2, vital volume 6 mL/kg, and 80 breaths per minute), and injection of epinephrine (0.02 mg/kg, intravenously), and 5% sodium bicarbonate (1 mmol/kg, intravenously). During the procedures, the rectal temperature of the animals was maintained within a range of 37.0 ± 0.5°C using an animal heating pad. CA was arbitrarily defined as mean arterial pressure (MAP) dropped to 25 mmHg, and restoration of ROSC was determined as the return of supraventricular rhythm with the MAP above 50 mmHg for 10 min. Ventilation was maintained until spontaneous breath recovery. Failure to restore spontaneous circulation within 15 minutes resulted in discontinuing resuscitation efforts. After ROSC, the rats were extubated and had a cut sutured.

Electroacupuncture Intervention

The locations of the acupoint related to rats were previously described.[15] The ST36 acupoint is located lateral and 5 mm below to the tibia anterior tubercle. An electrical stimulator provided the needle's electrical current (Suzhou Medical Appliance

Manufactory, SDZ-V, China). The frequency is 15 HZ, the current intensity is 1 mA, and the width is 0.4 ms, which causes a mild muscle twitch for a stimulation period of 30 minutes. Electroacupuncture was started immediately following the establishment of the CA/CPR rat and stimulated for another 30 min after 1 h. Rats in the EA-ST36 + MLA group received intraperitoneal injection of MLA (2.0 mg/kg, Tocris Bioscience, 1029, USA) 30 min prior to electroacupuncture stimulation. Rats in other groups received an intraperitoneal injection of phosphate-buffered saline (PBS) in an equal volume (Figure 1A).

Experimental Design

In a vivo experiment, to determine whether the EA-ST36 treatment exerts a neuroprotective effect by inhibiting microglial pyroptosis in an α7nAChR-dependent manner following CA/CPR, rats were randomly divided into 4 groups: sham surgery group (sham), CA/CPR group (CA/CPR), CA/CPR + EA-ST36-treated group (EA-ST36) and CA/CPR + EA-ST36 + methyllycaconitine citrate-treated group (EA-ST36 + MLA) (Figure 1B). In vitro experiment, to further confirm whether the α7nAChR suppressed microglial pyroptosis, primary cultured microglia were randomly divided into 3 groups: control (control), oxygen-glucose deprivation/reoxygenation (OGD/R), and OGD/R + PHA-543613 (OGD/R + PHA-543613). A co-culture system of neurons and microglia was established to study the neuroprotection effect of α7nAChR. The co-cultured neurons-microglia were randomly divided into 3 groups: control (control), OGD/R (OGD/R), and OGD/R + PHA-543613 (OGD/R + PHA-543613). All drugs were administered as previously described.[16–18]

Morris Water Maze

The Morris water maze was conducted to determine the spatial learning and memory abilities of rats (Taimeng, WMT-200B, China). The pool area was divided into four quadrants. The platform was positioned 2 cm below the water's

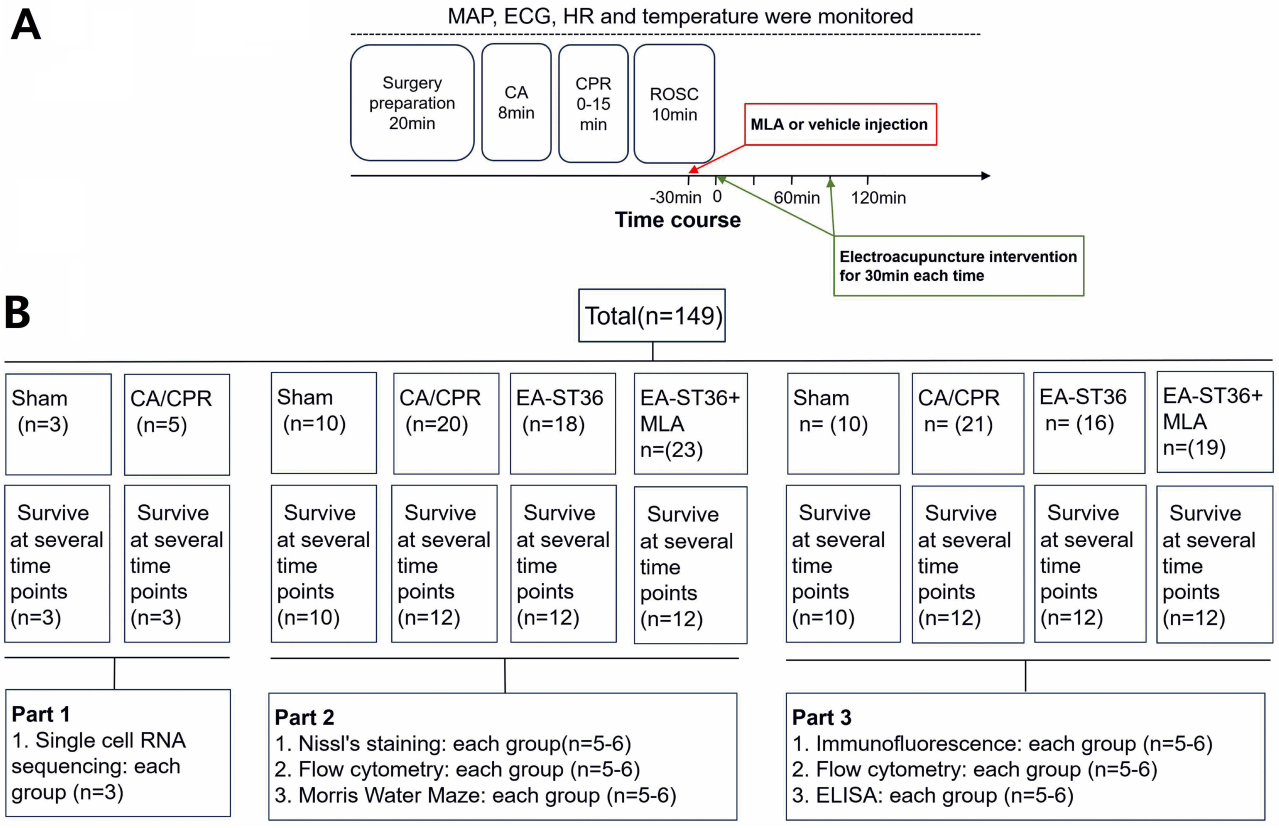

Figure 1 Diagrams of experimental procedures and groups. (**A**) Experimental procedures for drug delivery, and asphyxial cardiac arrest, and cardiopulmonary resuscitation, and ROSC. (**B**) The whole animal study is consisted of 3 parts. In part 1, Single-cell RNA sequencing was performed to explore in which cell types principally undergone the pyroptosis following CA/CPR. In part 2, rat's learning ability, and histological impairment in cardiac arrest model were assessed. In part 3, the occurrence of pyroptosis and neuroinflammation in cardiac arrest model was explored.

https://doi.org/10.2147/JIR.S525373

surface in the fourth quadrant. The rats were put into a quadrant opposite the platform, and the escape latencies time was recorded. If the rats were not able to access the platform within 60 s, they would be guided to the platform and kept there for 10 s. Each rat had three training trials were operated for per day for 3 d. The platform was removed on 7 d. The dwell time in the target quadrant was recorded in 60 s.

Single-Cell RNA Sequencing

The single-cell RNA sequencing was completed by LC Biological Technology Co. (Hangzhou, China). Briefly, single-cell suspension of brain tissue was prepared from each sample, cell quantity and viability were measured according to the manufacturer's instructions, and a cell suspension volume equivalent to 10000 target cells was used for further processing. Preparation of gel beads in emulsion and libraries was performed with Chromium Controller and Single-Cell Gene Expression v2 Chemistry (10× Genomics), according to the Chromium Single-Cell 3' Reagent Kits User Guide provided by the manufacturer. Libraries' quality and quantity were verified with a High-Sensitivity DNA Kit (Agilent Technologies, USA) on a Bioanalyzer (Agilent Technologies, 2100, USA). Gene expression measurements for each cell were normalized by the total number of transcripts, multiplied by a default scale factor, and the normalized values were log-transformed ("LogNormalize" method).

Primary Cell Isolation and Co-Culture of Microglia and Neuron

Primary cell isolation and co-culture of neuron and microglia were performed as previously described.[16–18] For primary microglia isolation, mixed primary cells were isolated from the cerebral cortex of 1-day-old neonatal rat. After removing the meninges and hippocampus, the tissues were cut into pieces and performed enzymatic digestion. Then the cell suspension was passed through a 70-mm nylon mesh cell strainer and were seeded into the poly-L-lysine (Gibco, A3890401, USA) coated cell culture flask in Dulbecco's modified Eagle's medium (DMEM, Gibco,11965092, USA) containing 10% fetal bovine serum (FBS, Gibco, A5670701, USA) and 1% antibiotics (penicillin and streptomycin, Gibco, 15140122, USA) at 37°C with 5% CO_2. Microglia were harvested by mild shaking at 220 r/min for 1 h and were shifted into a cell culture dish. The purity of the microglia was confirmed by using immunofluorescence staining of Iba-1. For primary neuron isolation, the hippocampus of E17–E19 rat embryos were used to isolate primary neurons. The primary neurons were seeded into the poly-L-lysine coated petri dish. Cells were seeded in Neurobasal medium (Gibco, 12348017, USA) containing 2% B27 (Gibco, 17504044, USA), 1% glutamine (Gibco, A2916801, USA), 1% antibiotics (penicillin and streptomycin, Gibco, 15140122, USA) and cultured at 37°C with 5% CO_2. For the co-culture of microglia and neurons, the microglia (neurons: microglia = 2:1) were seeded to the inserts of Transwell (Thermo Fisher Scientific, 140620, USA) at 2 d after the neurons were seeded.

Oxygen Glucose Deprivation/Reoxygenation (OGD/R) Model

The cells were transferred to a serum, and glucose-free Dulbecco's modified Eagle's medium (DMEM, Gibco, 11966025, USA) and were then cultured in a humidified hypoxic chamber (Billups, MIC-101, USA), which contained mixed gas (5% CO_2 and 95% N_2) at 37°C. The Oxygen-glucose deprivation (OGD) treatment was last for 4 h (microglia) or 1 h (neuron). In the OGD/R+PHA-543613 group, PHA-543613 (100 μM, Tocris Bioscience, 3092, USA) was added into the cultured medium 24 h before OGD treatment. Other groups received an equal volume of phosphate-buffered saline (PBS). To prevent medications activating a7nAChR in neurons, neurons and microglia were incubated separately during the drug treatments and OGD. After OGD treatment, the cells were treated with reoxygenation for an additional 24 h.

Nissl Staining

Rats were anesthetized as previously described following the Morris water maze test, then they were perfused with saline and 4% paraformaldehyde. After being submerged in 4% paraformaldehyde for 16 h, the specimens were dehydrated using gradients sucrose of 10%, 20%, and 30%. The coronal brain sections were obtained using a frozen slicer (Leica, CM 1950, Germany). Brain sections were dried in 70%, 80%, and 90% alcohol for 2 minutes and in 100% alcohol for 10 minutes, after which it was dyed with tar purple (Solarbio, G1430, China).

Immunofluorescence

Brain sections were prepared as described above at 2 d following post-surgery. After blocking for 0.5 h in 5% BSA, brain sections were incubated with different primary antibodies below: rabbit anti-cleaved caspase-1 (Thermo Fisher Scientific, PA5-9939, USA), rabbit anti-α7nAChR (Abcam, ab216485, UK), mouse anti-Iba-1 (Abcam, ab283319, UK) for microglia, mouse anti-GFAP (Abcam, ab4648, UK) for astrocytes, mouse anti-NeuN (Abcam, ab104224, UK) for neurons, mouse anti-CD31 (Novus Biologicals, NB100-64796SS, USA) for endothelial cells and mouse anti-oligodendrocyte lineage transcription factor 2 (Olig2, Santa Cruz, sc-515947, USA) for oligodendrocytes, then these brain sections were incubated with donkey anti-rabbit Alexa Fluor 594 (Jackson ImmunoResearch, 711–585-152, USA) or goat anti-mouse Alexa Fluor 488 (Abcam, ab150113, UK) secondary antibodies, following by DAPI (Roche, 28718–90-3, Switzerland) counterstaining. Digital images of fluorescence were recorded using a confocal microscope (Nikon, A1, Japan) and analyzed by ImageJ (NIH, USA).

Flow Cytometry

The procedure of flow cytometry was performed as described previously.[5] After 2 d post-surgery, rats were anesthetized with injecting an overdose of pentobarbital sodium, then was perfused with ice-cold phosphate-buffered saline (PBS). The hippocampus was placed in ice-cold Hank's (Gibco, 14065056, USA) and mechanically isolated into a single-cell suspension by passage through a 70-μm cell strainer (Falcon, 352350, USA). For analysis of pyroptosis in microglia, the cells were labeled by the FAM-FLICA assay (Immunochemistry Technologies, 97, USA) to detect the caspase-1 activity. The cell viability was analyzed by the LIVE/DEAD Fixable Near-IR Dead Cell Stain (Life Technologies, L10119, USA) following the manufacturer's instructions. After a non-specific block with CD16/CD32 antibody, the cells were stained with CD45 APC antibody (Thermo Fisher Scientific, 17046182, USA) and CD11b PE antibody (Thermo Fisher Scientific, 12011082, USA). For detection of α7nAChR expression in microglia, the cells were stained with CD45 APC antibody (Thermo Fisher Scientific, 17046182, USA), CD11b PE antibody (Thermo Fisher Scientific, 12011082, USA) and α7nAChR antibody (Thermo Fisher Scientific, ANC-007, USA) following CD16/CD32 antibody blocking. A goat anti-Rabbit IgG Pacific Blue™ (Thermo Fisher Scientific, P-10994) was used as the secondary antibody. All gates were established using antibody isotype controls (provided by manufacturers). The cell samples were performed on a flow cytometer (SONY, SA3800, USA). The flow cytometry files were analyzed using Flowjo software (BD Science, V10, USA).

Western Blotting

For Western blotting analysis, cells were analysed in RIPA buffer (Beyotime Biotechnology, P0013B, China) containing a complete protease inhibitor cocktail (Roche, 04693132001, Switzerland). Samples were separated in a 10% SDS-PAGE and transferred to a PVDF membrane (Millipore, IPVH00010, USA). The PVDF membrane was incubated with different primary antibodies and the corresponding second antibody. Rabbit anti-α7nAChR antibody (Abcam, ab216485, UK), rabbit anti-NLRP3 antibody (Abcam, ab263899, UK), rabbit anti-caspase-1 (Abcam, ab179515, UK), rabbit anti-GSDMD (Abcam, ab239377, UK), mouse anti-β-actin (Abcam, ab8226, UK) were used as the primary antibodies. Goat anti-rabbit IgG-HRP (Cell Signaling Technology, 7074S, USA) or horse anti-mouse IgG-HRP (Cell Signaling Technology, 7076S, USA) was used as the second antibodies. Signals were detected with a scanner (Bio-Rad, Gel Doc XR+, USA).

ELISA

The pro-inflammatory cytokines interleukin-1β (IL-1β, R&D Systems, RLB00-1, USA) and interleukin-18 (IL-18, R&D Systems, DY521-05, USA) in the brain tissues or the cells culture supernatant following the different treatments were measured based on the enzyme-linked immunosorbent assay (ELISA) kit instructions.

MTS

After co-culturing microglia and neurons for 24 h following OGD treatment, the microglia were carefully removed. The viability of neurons was determined using the MTS (Promega, G5421, USA) kit following the assay kit instructions.

LDH

The lactate dehydrogenase (LDH, Beyotime Biotechnology, C0016, China) release of neurons was detected following the assay kit instructions after co-culturing microglia and neurons with OGD treatment as previously described.

Statistical Analysis

All data were presented as the means ± SD and analyses were performed using GraphPad Prism software (GraphPad 9.0, USA). The comparison between the two sets of data was performed using the *t*-test of independent samples; the comparison between the multiple data sets was performed using one-way ANOVA. $P<0.05$ was considered statistically significant.

Results

CA/CPR Triggered Microglial Pyroptosis in Brain

Single-cell RNA sequencing of rat brain and immunofluorescent co-localization were performed to explore in which cell types principally undergone the pyroptosis following CA/CPR. The data of single-cell RNA sequencing showed that the brain cells were clustered into different cell type. The cells were mainly divided into five groups, namely astrocytes, microglia, neurons, oligodendrocytes, and endothelial cells (Figure 2A). The pathway of pyroptosis is principally upregulated in microglia rather than neurons, astrocytes, oligodendrocytes, or endothelial cells (Figure 2B and C). The score of pyroptosis-related genes in microglia appeared elevated in the CA/CPR group compared to the sham group (Figure 2D). The Gene Ontology (GO)

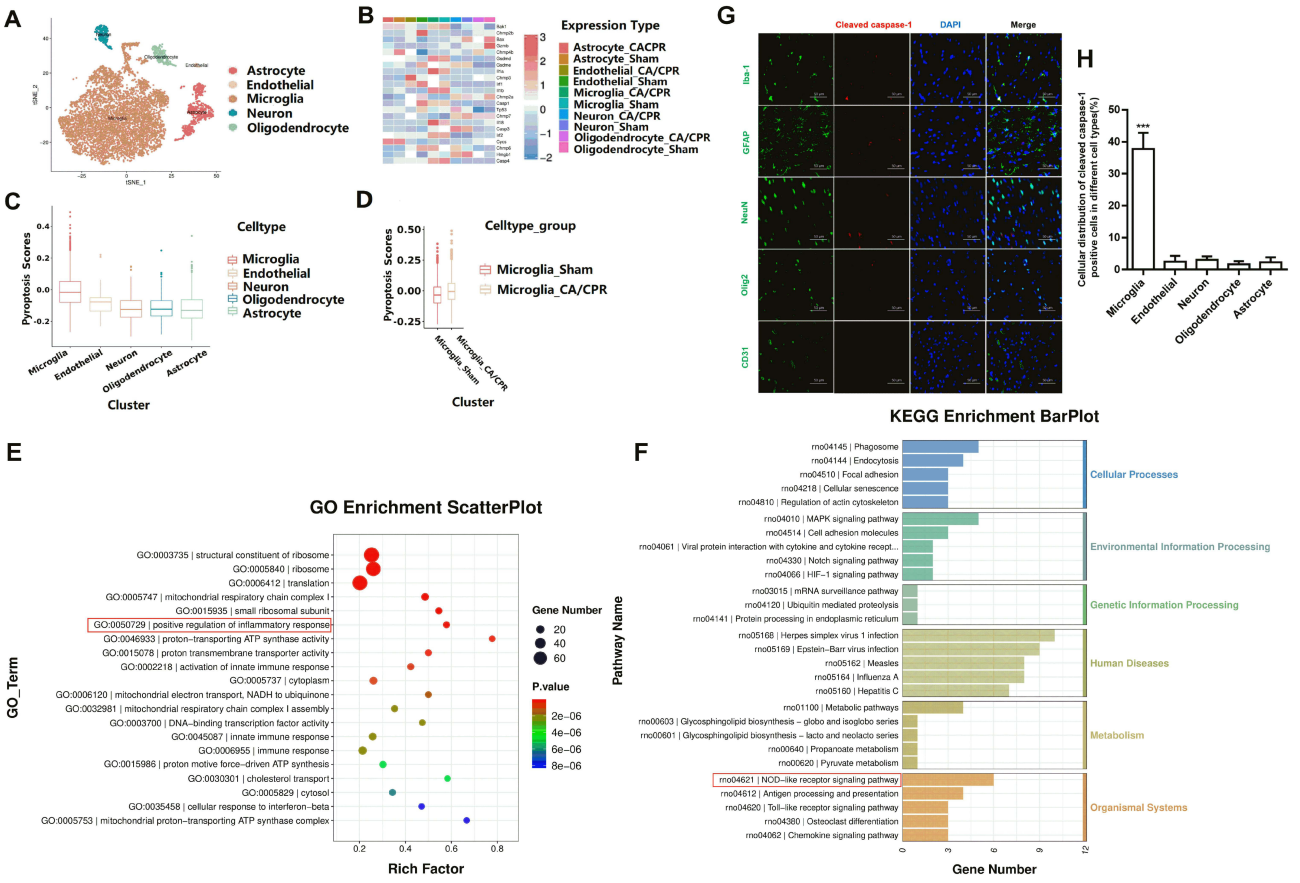

Figure 2 CA/CPR induced pyroptosis in microglia. (**A**) The tSNE nonlinear clustering was used to visualize the classification results of intracerebral cell subsets. (**B**) Stacked bar plot depicting the relative abundance of pyroptotic gene in each cell cluster. (**C**) The violin plots of the expression of pyroptosis marker molecules in each cell cluster. (**D**) The violin plots of pyroptosis marker molecules expression in microglia within each group. (**E**) The Gene Ontology (GO) enrichment analysis. (F)The Kyoto Encyclopedia of Genes and Genomes (KEGG) pathway enrichment analysis. (**G**) Immunofluorescence analysis of cleaved caspase-1 expression (red) in different cell types (green), including microglia (Iba-1), astrocyte (GFAP), neuron (NeuN), endothelial (CD31), and oligodendrocyte (Olig2) in CA/CPR rat (n=5). (**H**) Quantitative analysis of cleaved caspase-1 co-localization with cell-type markers.

enrichment results revealed that upregulation of biological processes related to inflammatory response (Figure 2E). The Kyoto Encyclopedia of Genes and Genomes (KEGG) pathway enrichment analysis further highlighted activation of the NOD-like receptor signaling pathway (Figure 2F). By using immunofluorescent, the colocalization analysis of cleaved caspase-1 with specific cell markers (Iba-1 for microglia, NeuN for neurons, GFAP for astrocytes, CD31 for endothelial cells, and Olig2 for oligodendrocytes) revealed that the number of cleaved-caspase-1 positive microglia were significantly higher compared to other cleaved caspase-1 positive cell types (Figure 2G and H).

α7nAChR is Involved in the Neuroprotective Effects of EA-ST36 to Improve the Spatial Learning and Memory in CA/CPR Rats

After establishing the Rat Model of Asphyxial Cardiac Arrest, the spatial learning and memory abilities of rats were monitored. The escape latency of rats was determined at 4, 5, and 6 d. With the increase in training times and days, the escape latency of rats in each group was gradually shortened. The escape latency of rats in the CA/CPR group was longer compared with the rats in sham surgery group during consecutive tests. The escape latency of rats was significantly shortened in the EA-ST36 group compared with the rats in the CA/CPR group in the 4, 5 and 6 d (Figures 3A and B). The time in target quadrant was determined at 7 d. The time of CA/CPR rat stayed in the target quadrant were shortened significantly compared to those with sham surgery or EA-ST36 treated rats (Figure 3C). In contrast, the EA-ST36+MLA treatment was poorly decreased the escape latency or improved the time in target quadrant comparison with rats in EA-ST36 group. The data of water maze test indicated that EA-ST36 attenuated the impairments of learning and memory impairments in the CA/CPR rats depend on α7nAChR.

EA-ST36 Reduced Neuron Injury in CA/CPR Rats Depend on α7nAChR

The neuron injury was analyzed by flow cytometry after 2 d. As shown in (Figure 3D), the hippocampal cells apoptotic rate was determined by using Annexin V-FITC/PI double staining. The early apoptotic hippocampal cell was labeled by Annexin V-FITC, and the necrosis hippocampal cell was labeled by PI. After the CA/CPR, the apoptotic rate of the hippocampal cells of rats obviously increased compared with the rats in the sham surgery group. The apoptotic rate of hippocampal cells of EA-ST36 treated rats was significantly lower compared to CA/CPR rats. The EA-ST36+MLA treatment was failed to decrease the apoptotic rate of the hippocampal cells of rats compared with the effect of EA-ST36 treatment. The histopathological changes in the hippocampus area were evaluated using Nissl's staining. As shown in Figure 3E, on the 7 d following CA/CPR, the rats in the sham surgery group showed a normal hippocampal structure, the neurons were tightly connected, and the basement membrane was intact. The neurons of rats in the CA/CPR or EA-ST36 +MLA group showed obvious changes in the morphology, which appeared as massive cell loss in the hippocampal CA1 region, dilated intercellular space, cellular edema, and disorderly arrangement. There were more surviving neurons of rats in the EA-ST36 group than those in the CA/CPR and EA-ST36+MLA groups. The EA-ST36 therapy significantly improved this histopathological lesion compared with the rats in CA/CPR group, which showed an obvious reduction of necrotic cell number and close to normal intercellular space and nucleus staining. These results suggested α7nAChR is involved in the neuroprotective effect of EA-ST36 on the hippocampal cells of the CA/CPR rat.

EA-ST36 Inhibited the Microglial Pyroptosis and Consequential Neuroinflammation Following CA/CPR Through Activating α7nAChR

We speculated that EA-ST36 improved memory and cognitive ability and reduced neurons injury by alleviating neuroinflammation against the microglial activation and pyroptosis through activating α7nAChR in CA/CPR rats. Hence, flow cytometry and ELISA were employed to investigate the effect of EA-ST36 on inhibition of microglial activation and pyroptosis. The flow cytometry data showed that activated and pyroptotic microglia populations increased in CA/CPR rats compared with the sham surgery rats after 2 d. The EA-ST36 treatment significantly reduced the number of activated and pyroptotic microglia compared to rats in the CA/CPR group. Nevertheless, these inhibiting effects of EA-ST36 on microglial activation and pyroptosis could be reversed by the administration of MLA, the α7nAChR antagonist (Figure 4A–E). The results from ELISA showed that EA-ST36 significantly suppressed the levels of IL-1β and

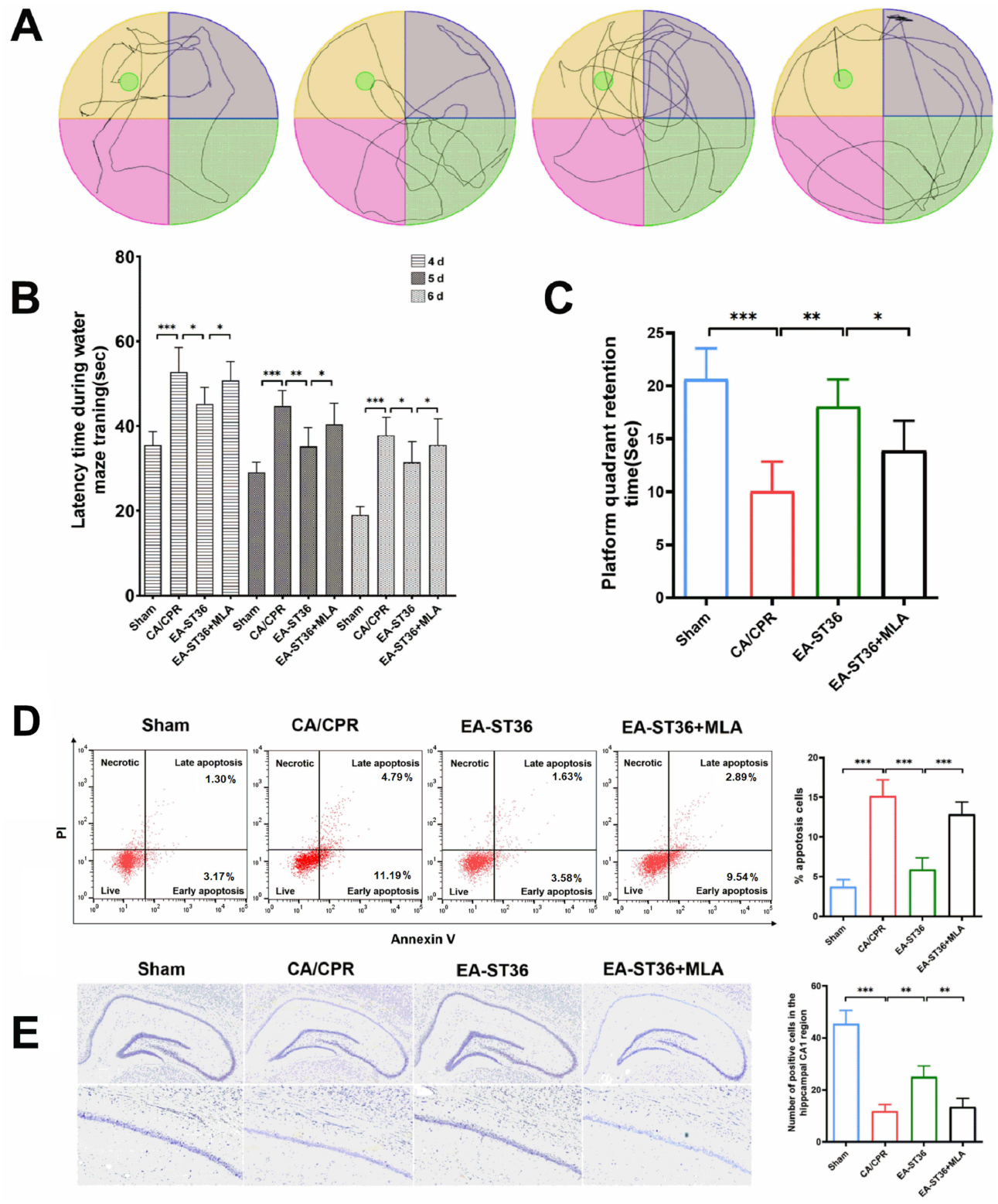

Figure 3 α7nAChR is involved in the neuroprotective effects of EA-ST36 to improve the spatial learning and memory and reduce the neuron injury in CA/CPR rats. (**A**) Representative graphs of spatial search tracks in MWM. (**B**) The escape latency in searching the hiding platform. (**C**) The time spent in the target quadrant during the probe trial. (**D**) The neuropathological damage characterized by the changes in Nissl staining. (**E**) The apoptosis analysis of hippocampal cells. All data were presented as the mean ± SD. **P* < 0.05, ***P* < 0.01, ****P* < 0.001. (n=5-6 per group).

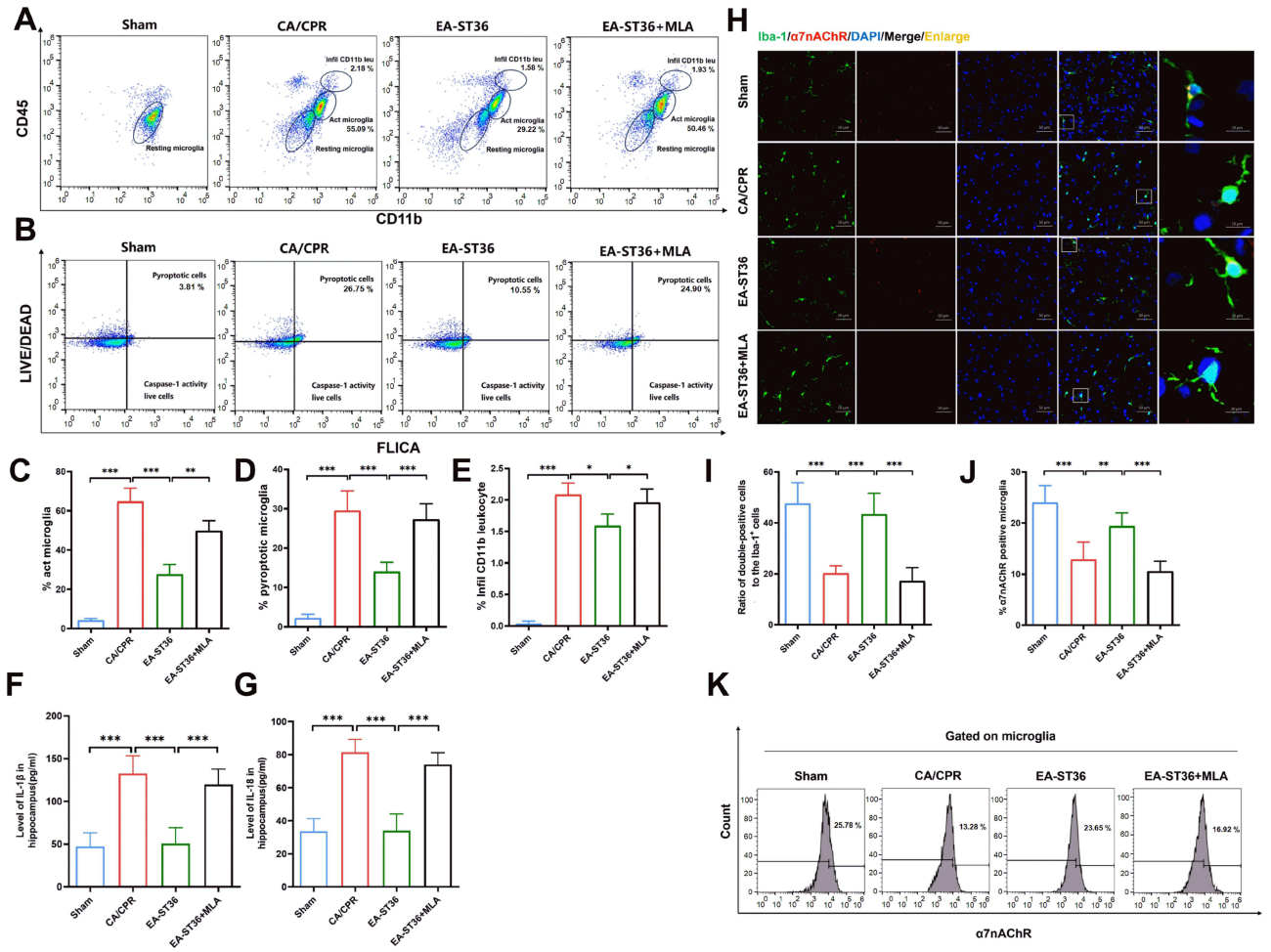

Figure 4 EA-ST36 inhibited the microglial activation and pyroptosis and consequential neuroinflammation following CA/CPR depend on α7nAChR activation. (**A–E**) Flow cytometry analysis of resting microglia ($CD45_{low}$, $CD11b^{+}$), activated microglia ($CD45_{int}$, $CD11b^{+}$), pyroptotic microglia ($FLICA_{high}$, $LIVE/DEAD_{high}$), and infiltrating leukocytes population ($CD45_{high}$, $CD11b^{+}$). (**F**) The levels of IL-1βin hippocampus. (**G**) The levels of IL-18 in hippocampus following CA/CPR. (**H**) Immunofluorescence analysis of α7nAChR (red) expression in microglia (green). (**I**) Quantification of fluorescence intensity. (**J-K**) Flow cytometry analysis α7nAChR expression in microglia. All data were presented as the mean ± SD. *P < 0.05, **P < 0.01, ***P < 0.001. (n=5-6 per group).

IL-18 after 2 d in hippocampus and the administration of MLA could significantly reverse the inhibition effect of EA-ST36 on IL-1β and IL-18 level (Figure 4F and G). Subsequently, we investigated whether the EA-ST36 promoted expression of α7nAChR in microglia in the brain following CA/CPR. Both the data of flow cytometry and immunofluorescence suggested that the α7nAChR expression on the microglia of CA/CPR rats were decreased significantly compared to sham surgery rats. The α7nAChR expression on the microglia of EA-ST36 rats were increased significantly compared to CA/CPR rats. This promoting effect of EA-ST36 on α7nAChR could be reversed by the administration of MLA in microglia of rats (Figure 4H–K).

Activation of α7nAChR Attenuated Microglial Pyroptosis and Its Neurotoxic Effects

To further confirm the inhibitory effect of α7nAChR on microglial pyroptosis in CA/CPR brain injury, the primary rat microglia oxygen-glucose deprivation/reoxygenation (OGD/R) model was established with α7nAChR agonist (PHA-543613) intervention. The flow cytometry data showed that the pyroptotic microglia populations in the OGD/R group increased significantly compared to the control group, while α7nAChR agonist (PHA-543613) intervention significantly inhibited pyroptotic microglia populations (Figure 5A and B). The ELISA data showed that the concentrations of IL-1β and IL-18 in the supernatant of the microglial culture medium in the OGD/R group were significantly increased compared with the control group, indicating the activation of the microglial pyroptosis downstream effector. The

https://doi.org/10.2147/JIR.S525373

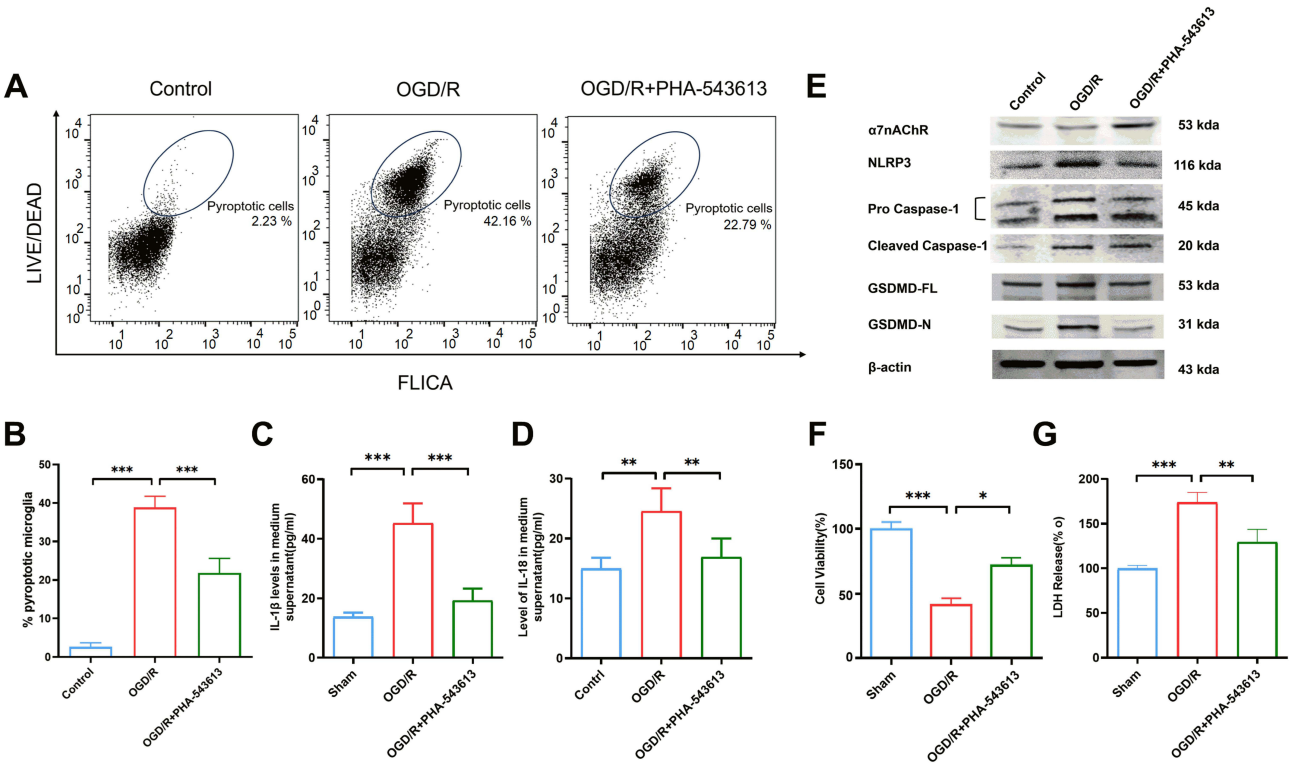

Figure 5 Activation of α7nAChR inhibited microglial pyroptosis and attenuated its neurotoxic effects after OGD/R in vitro.(**A and B**) Flow cytometry analysis of pyroptotic microglia ($FLICA_{high}$, $LIVE/DEAD_{high}$). (**C**) ELISA analysis the levels of IL-1β in the supernatant of the microglial culture medium. (**D**) ELISA analysis the levels of IL-18 in the supernatant of the microglial culture medium. (**E**) Western blot analysis of the expression levels of a7nAChR, NLRP3, caspase-1 and GSDMD protein in primary microglia. (**F**) MTS assay analysis of neuronal viability after co-culturing microglia and neuron. (**G**) LDH assay analysis of neuronal viability after co-culturing microglia and neuron. All data were presented as the mean ± SD. *$P < 0.05$, **$P < 0.01$, ***$P < 0.001$. (n=3-6 per group).

concentrations of IL-1β and IL-18 in the supernatant of microglial culture medium in the OGD/R+PHA-543613 group were significantly decreased compared with the OGD/R group (Figure 5C and D). The Western blotting results indicated that the NLRP3, cleaved caspase-1, and N-GSDMD expression were increased, and the α7nAChR expression was decreased in microglia of OGD/R group, compared with these in microglia of control group. Remarkably, the α7nAChR expression upregulated and the NLRP3, cleaved caspase-1, and N-GSDMD expression were downregulated in microglia of the α7nAChR agonist (PHA-543613) intervention group, compared with these in microglia of OGD/R group (Figure 5E). To assess the impact of microglial pyroptosis on neuronal survival, a Transwell co-culture system was used to co-culture primary microglia and neurons in different treatment groups, and the neuronal viability and LDH release were detected. The results showed that the viability of neurons was decreased, and the release of LHD was increased significantly in the OGD/R-treated co-culture group, compared with these in control group. The neuronal viability was significantly enhanced, and the release of LHD was significantly reduced in the OGD/R+PHA-543613 group compared with the OGD/R group (Figure 5F and G). Together, these results demonstrated that microglial pyroptosis was detrimental to neuronal survival following OGD/R, while activation of α7nAChR effectively suppressed the signaling pathways of pyroptosis in microglia and rescued neuronal death.

Discussion

Pyroptosis is a pro-inflammatory form of programmed cell death triggered by NOD-, LRR- and pyrin domain-containing protein 3 (NLRP3) inflammasome and executed by the caspase-1 and transmembrane pore-forming proteins known as gasdermin D (GSDMD).[19] Pyroptosis responds to microbial infection, endogenous danger signals, and environmental stimuli, which contribute to innate immune defense and homeostatic maintenance.[20] Canonical pyroptosis causes cell lysis and mediates proteolytic cleavage and release of inflammatory cytokine. More recently, researchers have revealed that pyroptosis plays critical roles in CNS diseases and varied brain regions or cell types may be affected by pyroptosis in

different manners.[20] In this study, the 8-min asphyxia CA/CPR rat model was exploited to reproduce the pathophysiology of hypoxic-ischemic encephalopathy and histological injury similar to asphyxial humans. The brain tissue of the CA/CPR rat was analyzed by single cell RNA sequencing. The data revealed that the signal pathway of pyroptosis was mainly upregulated in microglia rather than neurons, astrocytes, endothelial cells, or oligodendrocytes following CA/CPR. The immunofluorescence results confirmed that the expression of cleaved caspase-1 mainly increased in the microglia of rats rather than other types of cells in the brain following CA/CPR. As the resident immunocyte of brain, microglia are initiated in inflammatory cascades reaction and drive pathological progression in cerebral ischemic injury.[21] Previous study indicated that the microglial pyroptosis-caused neuroinflammation aggravated brain damage. Therefore, the occurrence of microglial pyroptosis following CA/CPR provides a new therapeutic target for the suppression of neuroinflammation to create a favorable immunological microenvironment that is conducive to neuron survival.

Despite considerable endeavors that have been done, the curative effects of CA/CPR-induced global cerebral ischemic injury are still limited. Based on behavioral experiments in various cerebral ischemic animal models and clinical studies, it has been demonstrated that EA treatment could remarkably improve cognitive impairment without causing severe side effects.[22] However, as yet, little is known about the molecular mechanisms of EA treatment in neuroprotection.

It is widely recognized that different acupoints with acupuncture produce varying outcomes, even for the same disease.[23] Noteworthy, ST36 acupoint shows more pronounced anti-inflammatory properties through stimulating the vagus nerve to activate α7nAChR in cholinergic pathway than other conventional acupoints.[24] Studies showed that a reduction in inflammatory factor production could be achieved by activating α7nAChR in various brain injury models. Wang et al[25] found that an α7nAChR agonist markedly reduced proinflammatory cytokine expression in an ischemic stroke rat model. Cortes et al[26] found that employing an α7nAChR antagonist exacerbated the microglial inflammatory response in a vitro model of developmental programming of neuroinflammation induced by lipopolysaccharide (LPS). In this study, our data showed that α7nAChR is involved in the neuroprotective effects of EA-ST36 to improve the spatial learning and memory through attenuating neuron injury in CA/CPR rats. Hence, we wonder whether the neuroprotection effect of EA-ST36 in CA/CPR rats depends on its anti-neuroinflammatory properties against microglial pyroptosis through activating α7nAChR. We found that EA-ST36 significantly inhibited the activation and pyroptosis of microglia in the hippocampus of CA/CPR rats. Jiang et al[27] found that over-activated microglia may finally execute pyroptosis in response to injury and infection, which successively induce persistent neuroinflammation. In addition, our data indicated that EA-ST36 significantly reduced leucocyte infiltration and the level of IL-1β and IL-18 in the hippocampus of CA/CPR rats. The inhibition of microglial pyroptosis accompanied by the reduction of inflammatory factors and leucocyte infiltration suggested that the EA-ST36 prevented the pyroptotic microglia-induced inflammatory response following post-cardiac arrest. By inhibiting in the expression of α7nAChR, the effect of suppression on microglial activation and pyroptosis with EA-ST36 was weakened significantly. These data indicated that EA-ST36 had potent anti-neuroinflammatory potential by suppressing the microglial pyroptosis in CA/CPR rats, and the anti-neuroinflammatory property of EA-ST36 was α7nAChR-dependent.

Previous studies have suggested that NLRP3 is critical in mediating pyroptosis.[28] Gustin et al[29] found that NLRP3 primarily functioned in microglia and could not regulate the activity of astrocytes. Zhu et al[30] showed that blocking NLRP3 expression increased the survival rate and enhanced the learning memory in mice while also reducing activated microglia and lowering proinflammatory factor production. To confirm the inhibitory effect of α7nAChR on the expression of NLRP3 and its downstream pyroptosis related molecules in microglia, the OGD/R model was conducted. We observed that activating α7nAChR by its agonist inhibited OGD/R-induced microglial pyroptosis and the expression of NLRP3, cleaved caspase-1 and N-GSDMD and the release of proinflammatory factor in microglia. To evaluate the impact of microglial pyroptosis on neuronal survival, the microglia-neurons co-culture system was established. It showed that activating a7nAChR attenuated pyroptotic microglia-caused neuronal injury. Together, the a7nAChR was involved crucially in the neuroprotection of EA-ST36 treatment against microglial pyroptosis in CA/CPR rats (Figure 6).

However, there are a few limitations in our study. While our study demonstrates that EA-ST36 effectively attenuates microglial pyroptosis and neuroinflammation via α7nAChR activation following CA/CPR, the question of whether other acupoints may offer comparable neuroprotective effects remains unexplored. The future study design will include parallel

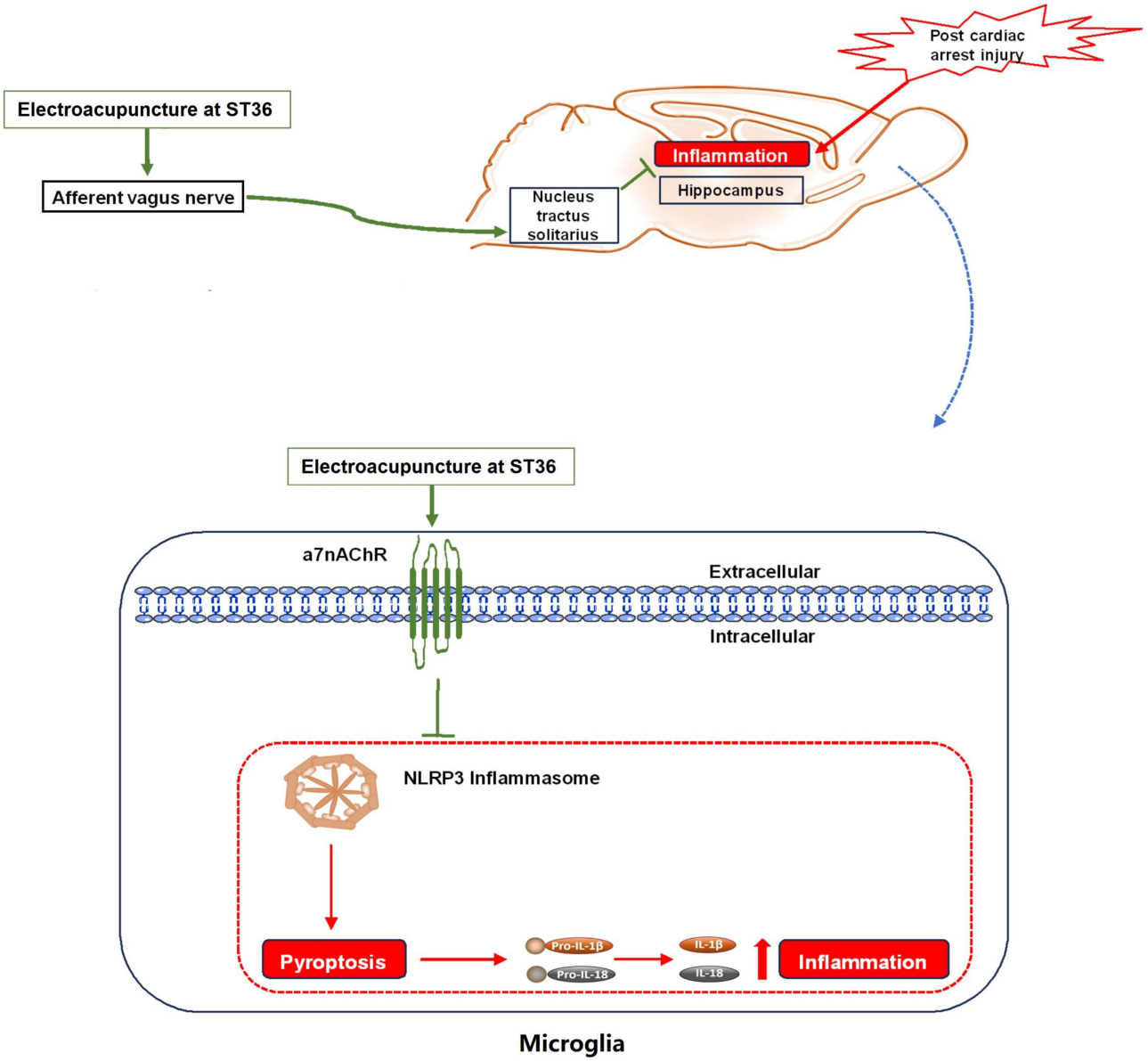

Figure 6 Diagrammatic representation of the neuroprotective mechanisms of EA-ST36 following CA/CPR. EA-ST36 attenuated brain injury and neuroinflammation through α7nAChR-mediated inhibition of microglial pyroptosis in a Rat Model of Asphyxial Cardiac Arrest.

EA interventions at acupoints such as ST36, LI4, GV20, and PC6 in the CA/CPR model, combined with behavioral, molecular, and histological analyses to determine acupoint specificity and mechanism of neuroprotective effects and their roles in α7nAChR activation. In addition, in this study, microglial α7nAChR is not directly activated in vivo to mimic the effect of acupuncture which would help establish a causal link between α7nAChR and pyroptosis of microglia. The gene-editing tools (eg, AAV-mediated microglia-specific overexpression of α7nAChR) will be exploited in future study to mimic the effects of EA-ST36.

Conclusion

Our study revealed that EA-ST36 exerted neuroprotective effects with a potent anti-neuroinflammatory potential by suppressing microglial pyroptosis in a rat CA/CPR model, and these anti-neuroinflammatory properties are α7nAChR-dependent. These findings support EA-ST36 as a promising non-invasive intervention for post-cardiac arrest neuroinflammation and cognitive dysfunction. EA-ST36 target neuroinflammation may complement existing therapies and offer

a novel adjunct to improve neurological outcomes. However, translation of EA-ST36 intervention to clinical practice requires further validation.

Abbreviations

CA, cardiac arrest; OHCA, out-of-hospital cardiac arrest; CA/CPR, cardiac arrest/cardiopulmonary resuscitation, NTS, nucleus tractus solitarius. α7nAChR, α7nicotinic acetylcholine receptor, EA-ST36, electroacupuncture at ST36 acupoint, OGD/R, oxygen-glucose deprivation/reoxygenation, ELISA, enzyme-linked immunosorbent assay.

Acknowledgments

We thank colleagues and institutions that supported the authors of this study for their contributions.

Funding

The present study supported by the National Nature Science Foundation of China (No. 81971225), the Natural Science Basic Research Program of Shaanxi Province (No. 2023-JC-ZD-52), Special Project for Cultivating and Improving Military Traditional Chinese Medicine Service Ability (2023ZY028) and National Nature Science Foundation Promotion Programs of Tangdu Hospital (2021ZTXM-022).

Disclosure

The authors declare that there are no competing interests in this work.

References

1. Kiguchi T, Okubo M, Nishiyama C, et al. Out-of-hospital cardiac arrest across the World: first report from the International Liaison Committee on Resuscitation (ILCOR). *Resuscitation*. 2020;152:39–49. doi:10.1016/j.resuscitation.2020.02.044
2. Perkins GD, Callaway CW, Haywood K, et al. Brain injury after cardiac arrest. *Lancet*. 2021;398(10307):1269–1278. doi:10.1016/S0140-6736(21)00953-3
3. Sekhon MS, Stukas S, Hirsch-Reinshagen V, et al. Neuroinflammation and the immune system in hypoxic ischaemic brain injury pathophysiology after cardiac arrest. *J Physiol*. 2023.
4. Gou X, Xu D, Li F, Hou K, Fang W, Li Y. Pyroptosis in stroke-new insights into disease mechanisms and therapeutic strategies. *J Physiol Biochem*. 2021;77(4):511–529. doi:10.1007/s13105-021-00817-w
5. Chang Y, Zhu J, Wang D, et al. NLRP3 inflammasome-mediated microglial pyroptosis is critically involved in the development of post-cardiac arrest brain injury. *J Neuroinflammation*. 2020;17(1):219. doi:10.1186/s12974-020-01879-1
6. Ye A, Li W, Zhou L, Ao L, Fang W, Li Y. Targeting pyroptosis to regulate ischemic stroke injury: molecular mechanisms and preclinical evidences. *Brain Res Bull*. 2020;165:146–160. doi:10.1016/j.brainresbull.2020.10.009
7. Li J, Hao JH, Yao D, et al. Caspase-1 inhibition prevents neuronal death by targeting the canonical inflammasome pathway of pyroptosis in a murine model of cerebral ischemia. *CNS Neurosci Ther*. 2020;26(9):925–939. doi:10.1111/cns.13384
8. Sandroni C, Cronberg T, Sekhon M. Brain injury after cardiac arrest: pathophysiology, treatment, and prognosis. *Intensive Care Med*. 2021;47(12):1393–1414. doi:10.1007/s00134-021-06548-2
9. Hays SA. Enhancing rehabilitative therapies with vagus nerve stimulation. *Neurotherapeutics*. 2016;13(2):382–394. doi:10.1007/s13311-015-0417-z
10. Ay I, Napadow V, Ay H. Electrical stimulation of the vagus nerve dermatome in the external ear is protective in rat cerebral ischemia. *Brain Stimul*. 2015;8(1):7–12. doi:10.1016/j.brs.2014.09.009
11. Jiang T, Wu M, Zhang Z, et al. Electroacupuncture attenuated cerebral ischemic injury and neuroinflammation through alpha7nAChR-mediated inhibition of NLRP3 inflammasome in stroke rats. *Mol Med*. 2019;25(1):22. doi:10.1186/s10020-019-0091-4
12. Wang JY, Zhang Y, Chen Y, et al. Mechanisms underlying antidepressant effect of transcutaneous auricular vagus nerve stimulation on CUMS model rats based on hippocampal alpha7nAchR/NF-kappaB signal pathway. *J Neuroinflammation*. 2021;18(1):291. doi:10.1186/s12974-021-02341-6
13. Liu S, Wang Z, Su Y, et al. A neuroanatomical basis for electroacupuncture to drive the vagal-adrenal axis. *Nature*. 2021;598(7882):641–645. doi:10.1038/s41586-021-04001-4
14. Gao CJ, Niu L, Ren PC, et al. Hypoxic preconditioning attenuates global cerebral ischemic injury following asphyxial cardiac arrest through regulation of delta opioid receptor system. *Neuroscience*. 2012;202:352–362. doi:10.1016/j.neuroscience.2011.11.060
15. Wang MM, Zhang M, Feng YS, et al. Electroacupuncture inhibits neuronal autophagy and apoptosis via the PI3K/AKT pathway following ischemic stroke. *Front Cell Neurosci*. 2020;14:134. doi:10.3389/fncel.2020.00134
16. Dong Z, Peng Q, Pan K, Lin W, Wang Y. Microglial and neuronal cell pyroptosis induced by oxygen-glucose deprivation/reoxygenation aggravates cell injury via activation of the caspase-1/GSDMD signaling pathway. *Neurochem Res*. 2023;48(9):2660–2673. doi:10.1007/s11064-023-03931-x
17. Zhang Z, Qin P, Deng Y, et al. The novel estrogenic receptor GPR30 alleviates ischemic injury by inhibiting TLR4-mediated microglial inflammation. *J Neuroinflammation*. 2018;15(1):206. doi:10.1186/s12974-018-1246-x
18. Ma Z, Zhang Z, Bai F, Jiang T, Yan C, Wang Q. Electroacupuncture pretreatment alleviates cerebral ischemic injury through alpha7 nicotinic acetylcholine receptor-mediated phenotypic conversion of microglia. *Front Cell Neurosci*. 2019;13:537. doi:10.3389/fncel.2019.00537

19. Hu Y, Wang B, Li S, Yang S. Pyroptosis, and its role in central nervous system disease. *J Mol Biol*. 2022;434(4):167379. doi:10.1016/j.jmb.2021.167379
20. Lee SW, de Rivero Vaccari JP, Truettner JS, Dietrich WD, Keane RW. The role of microglial inflammasome activation in pyroptotic cell death following penetrating traumatic brain injury. *J Neuroinflammation*. 2019;16(1):27. doi:10.1186/s12974-019-1423-6
21. Man SM, Karki R, Kanneganti TD. Molecular mechanisms and functions of pyroptosis, inflammatory caspases and inflammasomes in infectious diseases. *Immunol Rev*. 2017;277(1):61–75. doi:10.1111/imr.12534
22. Hu J, Hu W, Tang L, Wang Y. Fundamental neurocircuit of anti-inflammatory effect by electroacupuncture stimulation identified. *Neurosci Bull*. 2022;38(7):837–839. doi:10.1007/s12264-022-00849-2
23. Tsai YT, Cheng CY. Electroacupuncture at the Dazhui and Baihui acupoints and different frequencies (10 and 50 Hz) protects against apoptosis by up-regulating ERK1/2-mediated signaling in rats after global cerebral ischemia. *Iran J Basic Med Sci*. 2024;27(6):706–716. doi:10.22038/IJBMS.2024.72279.15716
24. Liang H, Ruan S, Wang F, et al. Electroacupuncture alleviates neurological function via activating the Yap-OPA1 axis and mitochondrial fusion in rats with cerebral ischemia-reperfusion injury. *Zhen Ci Yan Jiu*. 2023;48(11):1088–1094. doi:10.13702/j.1000-0607.20230345
25. Wang YY, Lin SY, Chang CY, et al. alpha7 nicotinic acetylcholine receptor agonist improved brain injury and impaired glucose metabolism in a rat model of ischemic stroke. *Metab Brain Dis*. 2023;38(4):1249–1259. doi:10.1007/s11011-023-01167-w
26. Cortes M, Cao M, Liu HL, et al. alpha7 nicotinic acetylcholine receptor signaling modulates the inflammatory phenotype of fetal brain microglia: first evidence of interference by iron homeostasis. *Sci Rep*. 2017;7(1):10645. doi:10.1038/s41598-017-09439-z
27. Jiang W, Liu Z, Wu S, et al. Neuroprotection of Emodin by Inhibition of Microglial NLRP3 Inflammasome-Mediated Pyroptosis. *J Integr Neurosci*. 2023;22(2):48. doi:10.31083/j.jin2202048
28. Coll RC, Schroder K, Pelegrin P. NLRP3 and pyroptosis blockers for treating inflammatory diseases. *Trends Pharmacol Sci*. 2022;43(8):653–668. doi:10.1016/j.tips.2022.04.003
29. Gustin A, Kirchmeyer M, Koncina E, et al. NLRP3 Inflammasome is expressed and functional in mouse brain microglia but not in astrocytes. *PLoS One*. 2015;10(6):e0130624. doi:10.1371/journal.pone.0130624
30. Zhu J, Zhou F, Zhou Q, et al. NLRP3 activation in microglia contributes to learning and memory impairment induced by chronic lead exposure in mice. *Toxicol Sci*. 2023;191(1):179–191. doi:10.1093/toxsci/kfac115